

The Corrosion Inhibition Effect of Pyrrole Derivatives on Carbon Steel in 1.0 M HCl

H.S.Gadow^{1,*}, H. M. Dardeer²

¹ Higher Institute for Engineering and Technology, New Demietta.

² Chemistry Department, Faculty of Science, South Valley University, Qena, Egypt

*E-mail: hsgado73@gmail.com

Received: 27 March 2017 / Accepted: 14 May 2017 / Published: 12 June 2017

The inhibition effect of new pyrrole derivatives, namely, 13-((4-aminophenyl)sulfonyl)-10,11-dihydro-9H-9,10-[3,4]epipyrrolo anthracene-12,14(13H,15H)-dione (**1**), anthracen-9(10H)-ylidenehydrazine(**2**), (11S,15R)-13-(anthracen-9(10)-ylideneamino)10,11-dihydro-9H-9,10 [3,4]epipyrroloanthracene-12,14-(13H,15H)-dione (**3**), 1,6-bis-(N-hexachloro-5-norbornene-2,3-dicarboximidyl) hexane (**4**) and N-Phenylsulfonyloxy-hexachloro-5-norbornene-2,3-dicarboximide (**5**), against the corrosion of carbon steel in 1.0 M HCl solution has been systematically studied by electrochemical measurements (potentiodynamic polarization measurements –impedance spectroscopy-electrochemical frequency modulation). The results of Potentiodynamic polarization indicate that all pyrrole derivatives are Mixed type inhibitors. Among the studied compounds, exhibited the best inhibition activity of 82.8% at 21×10^{-6} M from compound (**1**). The chemical structure of the synthesized compounds was established by proton and carbon thirteen nuclear magnetic resonance (¹H-NMR), (¹³C-NMR), Fourier transform infrared (FTIR) and mass spectroscopy. Solution analysis (UV–visible spectrophotometric method- Fourier transform infrared [FTIR]) support the above inferences.

Keywords: carbon steel; corrosion inhibition; pyrrole derivatives; HCl; EFM; FTIR

1. INTRODUCTION

Hydrochloric acid is commonly used for the removal of rust and undesirable scale in the metal working, cleaning of heat exchangers and boilers. Blistered coating happens because of over-pickling of metal. Now the formation of protective film on the steel surface and characterization of metal surface is the major subject of interest. Carbon steel is among the most widely used engineering materials such as marine applications, nuclear and fossil fuel power plants, metal-processing

equipment, chemical processing, transportation, pipelines, mining and construction. The alloys of iron as construction materials in industrial sectors has become a great challenge for corrosion engineers or scientists nowadays [1]. Corrosion inhibitors consider very important for protecting many metals and alloys. This leads to study the use of organic compounds as corrosion inhibitors. Adsorption of organic molecules on the surface of metals depend on their molecular structures, surface charge density [2,3]. Most of the organic compounds containing nitrogen, sulphur, oxygen with aromatic and heterocyclic rings through which they are adsorbed on the metal surface have been reported to be effective inhibitors for the corrosion of steel in acid media [4-8]. The choice of appropriate inhibitors depends on the type and the concentration of acid, temperature, the presence of dissolved organic and/or inorganic substances even in minor amounts and on the type of metallic material which protected [9]. Pyrrole and its derivatives are present in nature. Pyrrole derivatives have different applications in medicinally active compounds containing cholesterol reducing agent, antifungicides, antibiotics[10]. Also pyrrole derivatives use as solvent for resin [11] , luminescence chemistry[12], catalyst for polymerization process[13], synthesis of alkaloids[14] and corrosion inhibitor[15,16] .

The aim of this paper is to synthesis of new pyrrole derivatives and explore, for the first time, the use of pyrrole derivatives as corrosion inhibitors for carbon steel in 1.0 M HCl medium. The choice of these compounds was based on the consideration that these organic compounds contain many π -electrons and hetero atoms like nitrogen, sulphur and oxygen atoms which induce greater adsorption on the steel surface compared with other organic inhibitors. The corrosion inhibitive activity of these organic compounds was examined successively via potentiodynamic polarization curves, electrochemical impedance spectroscopy (EIS), electrochemical frequency modulation (EFM), isotherm calculations, FT-IR and UV spectroscopy techniques.

2. EXPERIMENTAL

2.1 Materials

2.1.1 Electrode and solutions.

For electrochemical studies, the working electrode was cut from a carbon steel sheet its composition by (weight%) is 0.200 C, 0.350 Mn, 0.024 P, 0.003 Si and the balance Fe. The dimensions of the working electrode were 20 x20 x1 mm, and The exposed area of the electrode was abraded by different grades of emery papers (grades 320- 1200), then rinsed and dried according to the standard methods[17]. The corrosive medium (1.0 M HCl) was prepared from 37% hydrochloric acid (Merck) analytical grade chemical and double-distilled water.

2.1.2 Synthesis of inhibitors.

The recorded melting points were uncorrected and measured on Griffin melting point apparatus. All reagents and solvents were purchased from Acros Organics and used without further

purification. The reactions were monitored by thin layer chromatography (TLC) using silica gel G (Spectrochem Pvt. Ltd., Mumbai). Each new compounds were fully characterized by FT/IR-4100 type A Serial Number B117761016. Mass spectrometry (HP Model, MS 5988 and AmD 402/3, EI 70 ev), in addition to ^1H -NMR recorded on Bruker Avance II 400 NMR Spectrophotometer using DMSO and CDCl_3 as solvent, Chemical shifts are relative to TMS as internal reference.

Synthesis of 13-((4-aminophenyl)sulfonyl)-10,11-dihydro-9H-9,10-[3,4]epipyrroloanthracene-12,14(13H,15H)-dione (1).

(11S,15R)-9,10,11,15-tetrahydro-9,10-[3,4]furanoanthracene-12,14-dione (0.5 gm, 1.81 mmole) and sulfanilamide (0.31 gm, 1.81 mmole) was heated under reflux in DMF (10 ml) for 5 hrs. The reaction mixture was poured onto water, the solid formed was filtered off, then dried and crystallized from benzene to give 13-((4-aminophenyl)sulfonyl)-10,11-dihydro-9H-9,10-[3,4]epipyrroloanthracene-12,14 (13H,15H)-dione (0.68 gm, 1.58 mmole) (**1**) as white crystals and obtained in 85 % yield: mp: 306°C ; IR (KBr, cm^{-1}): indicates characteristic bands due to (νNH_2) at $3342, 3259\text{ cm}^{-1}$; ($\nu\text{C-H}$ aromatic) at 2969 cm^{-1} ; ($\nu\text{C=O}$'s) in the region $1776\text{--}1650\text{ cm}^{-1}$; ($\nu\text{C=C}$ aromatic) at 1610 cm^{-1} ; ($\nu\text{C-N}$) at 1317 cm^{-1} ; ^1H -NMR (400 MHz/DMSO) δ (ppm): 3.46 (s, 2H, 2CH sp^3); 4.89 (s, 2H, 2CH sp^3); 6.68-7.81 (m, 12H, arom.H+2H, NH_2); MS (EI, m/z): 430M+ corresponding to molecular formula ($\text{C}_{24}\text{H}_{18}\text{N}_2\text{O}_4\text{S}$). EA (%C, %H, %N,%S): Calc.: 66.99,4.18 ,6.51 ,7.45, Found, 66.96,4.21 ,6.48, 7.42.

Synthesis of anthracen-9(10H)-ylidenehydrazine (2).

A suspension of anthrone (0.5 gm., 2.6 mmol.) and hydrazine hydrate (3 mmol.) in toluene was refluxed for 6 hrs. After cooling; The precipitate formed was filtered off, dried and recrystallized from ethanol to give anthracen-9(10H)-ylidenehydrazine (0.42gm, 2.02 mmol.) as pale yellow crystals and obtained in 77.8% yield; m.p. $240\text{--}242^\circ\text{C}$; FT-IR (KBr, cm^{-1}): showed the presence of bands due to (νNH_2) at $3345, 3259\text{ cm}^{-1}$; ($\nu\text{C-H}$ aromatic) at 3080 cm^{-1} ; ($\nu\text{C-H}$ aliphatic) at 2900 cm^{-1} ; ($\nu\text{C=N}$) at 1704 cm^{-1} ; ^1H -NMR (300 MHz/ CDCl_3) indicated at δ 3.29 (s, 2H, CH_2); 4.79(s, 2H, NH_2); 7.12-8.34 (m, 8H, arom. H); MS (m/z): 208M+ corresponding to molecular formula ($\text{C}_{14}\text{H}_{12}\text{N}_2$); EA (%C, %H, %N); Calc.: 80.77, 5.77 ,13.46 ; Found, 80.75, 5.79,13.43.

Synthesis of (11S,15R)-13-(anthracen-9(10H)-ylideneamino)10,11-dihydro-9H-9,10-[3,4] epipyrroloanthracene-12,14-(13H,15H)-dione(3).

(11S,15R)-9,10,11,15-tetrahydro-9,10- [3,4]furanoanthracene-12,14-dione (0.5 gm, 1.81 mmole) was heated under reflux with anthracen-9(10H)-ylidenehydrazine (0.38 gm, 1.83 mmole) in DMF (20 ml) for 8 hrs., after cooling, the reaction mixture was poured onto ice-water. The solid formed was filtered off and recrystallized from toluene to afford compound (**3**) (0.76 gm) as white crystals and obtained in 90.5% yield; m.p. 320°C ; FT-IR (KBr, cm^{-1}): showed the presence of bands

due to (ν C-H aromatic) at 3262 cm^{-1} ; (ν C-H aliphatic) at 2923 cm^{-1} ; (ν C=O's) in the region $1776\text{--}1700\text{ cm}^{-1}$; (ν C=N) at 1620 cm^{-1} ; $^1\text{H-NMR}$ (400 MHz/DMSO) indicated at δ 3.44 (s, 2H, CH_2); 3.65 (s, 2H, 2CH sp^3); 4.87 (s, 2H, 2CH sp^3); 6.66–7.79 (m, 16H, arom. H); MS (m/z): 466M+ corresponding to molecular formula ($\text{C}_{32}\text{H}_{22}\text{N}_2\text{O}_2$). EA (%C, %H, %N); Calc.: 82.40, 4.72, 6.01; Found, 82.38, 4.75, 6.08.

Synthesis of 1,6-bis-(N-hexachloro-5-norbornene-2,3-dicarboximidyl) hexane (4).

A mixture of hexachloro-5-norbornene-2,3-dicarboxylic anhydride (0.5 gm, 1.35 mmole) was heated under reflux in toluene (20 ml) with hexamethylenediamine (1.35 mmole) for 4 hrs. After cooling the solid formed was collected and crystallized from benzene to give compound (**4**) (0.88 gm, 1.07 mmole) as white crystals and obtained in 80% yield: mp: $282\text{--}4^\circ\text{C}$; IR (KBr, cm^{-1}): indicated the presence of bands due to (CH_2) aliphatic at 2861 cm^{-1} and two bands for (ν C=O's) in the region $1781\text{--}1700\text{ cm}^{-1}$; (ν C=C aromatic) at 1598 cm^{-1} ; (ν C-N aliphatic) at 1155 cm^{-1} ; $^1\text{H-NMR}$ (400 MHz/DMSO) δ (ppm): 1.25 (m, 4H, 2 CH_2); 1.38 (m, 4H, 2 CH_2); 3.32 (t, 4H, CH_2); 4.08 (s, 4H, 4CH sp^3); MS (EI, m/z): 822M+ corresponding to molecular formula ($\text{C}_{24}\text{H}_{16}\text{N}_2\text{O}_4\text{Cl}_{12}$); EA (%C, %H, %N, Cl%); Calc.: 75.07, 1.96, 3.41, 51.76, Found, 75.04, 1.94, 3.38, 51.73

Synthesis of N-Phenylsulfonyloxy hexachloro-5-norbornene-2,3 dicarboximide (5).

An equimolar amount of N-hydroxy-hexachloro-5-norbornene-2,3-dicarboximide (1 gm, 2.59 mmole) and benzenesulfonyl chloride (2.95 mmole) were stirring in pyridine for 2 hrs. The solid formed was acidified with cold dilute HCl (1:1), the solid formed was filtered and dried. The target product (**5**) was crystallized from ethanol to give white crystals. (1.23 gm, 2.34 mmole) and obtained in 90.4% yield: mp: $282\text{--}4^\circ\text{C}$; IR (KBr, cm^{-1}): revealed the presence of band due to (ν C-H aromatic) at 3100 cm^{-1} and showed band for (ν C=O's) at 1754 cm^{-1} and two bands for ($\text{SO}_2\text{--O--}$) at $1397, 1195\text{ cm}^{-1}$; $^1\text{H-NMR}$ (400 MHz/DMSO) δ (ppm): 4.28 (s, 2H); 7.75–8.04 (m, 5H, arom. H); $^{13}\text{C-NMR}$ (400 MHz/DMSO) δ (ppm): 49.66 ($\text{sp}^3\text{--C-9}$); 50.11 ($\text{sp}^3\text{--C-14}$); 79.01 ($\text{sp}^3\text{--C-10}$); 79.26 ($\text{sp}^3\text{--C-13}$); 104.28 ($\text{sp}^3\text{--C-15}$); 125.96 (Ar-C-4); 128.84 (Ar-C-3); 129.41 (Ar-C-5); 130.47 (Ar-C-2); 131.48 (Ar-C-6); 133.95 (Ar-C-1); 136.77 ($\text{sp}^2\text{C-12}$); 148.78 ($\text{sp}^2\text{C-11}$); 163.75 (C-8, C=O); 166.40 (C-7, C=O); MS (EI, m/z): 526M+ corresponding to molecular formula ($\text{C}_{15}\text{H}_7\text{NO}_5\text{SCl}_6$); EA (%C, %H, %N, Cl%, S%): Calc.: 34.25, 1.33, 2.66, 40.44, 6.09 Found, 34.22, 1.31, 2.64, 40.41, 6.11.

2.2 Methods

2.2.1 Electrochemical measurements.

The electrochemical measurements were carried through conventional cell with three electrodes were used. The carbon steel was working electrode, the counter electrode was Pt wire electrode and the reference electrode is saturated calomel electrode (SCE). The electrochemical

measurements were performed through Gamry Instrument (PCI 300/4) Potentiostat / Galvanostat /ZRA. This instrument inclusive a Gamry framework system based on the ESA 400. The applications of Gamry inclusive DC105 software for potentiodynamic polarization measurements, EFM 140 software for electrochemical frequency modulation measurements along with a computer for collecting data and EIS300 software for electrochemical impedance spectroscopy . For plotting, graphing, and fitting data, Echem Analyst 6.03 software was used.

2.2.2 FTIR analysis.

FTIR analysis was carried out to determine the functional groups present in the solutions of the inhibitors ($21 \times 10^{-6} \text{M} + 1.0 \text{ M HCl}$) and the functional groups present in the inhibitors ($21 \times 10^{-6} \text{M} + 1.0 \text{ M HCl}$) after the specimen of carbon steel immersed

2.2.2.3 UV –visible spectroscopy.

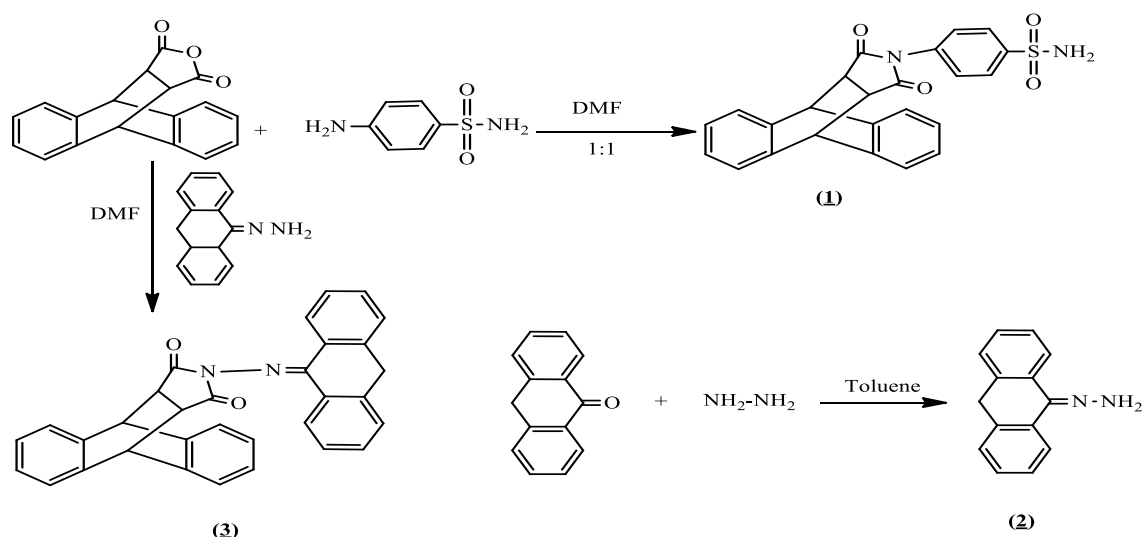
The UV-Visible absorption spectra of 1.0 M HCl solution containing $21 \times 10^{-6} \text{M}$ for different compounds before and after immersion of the carbon steel for 24 h were studied .

3. RESULTS AND DISCUSSION

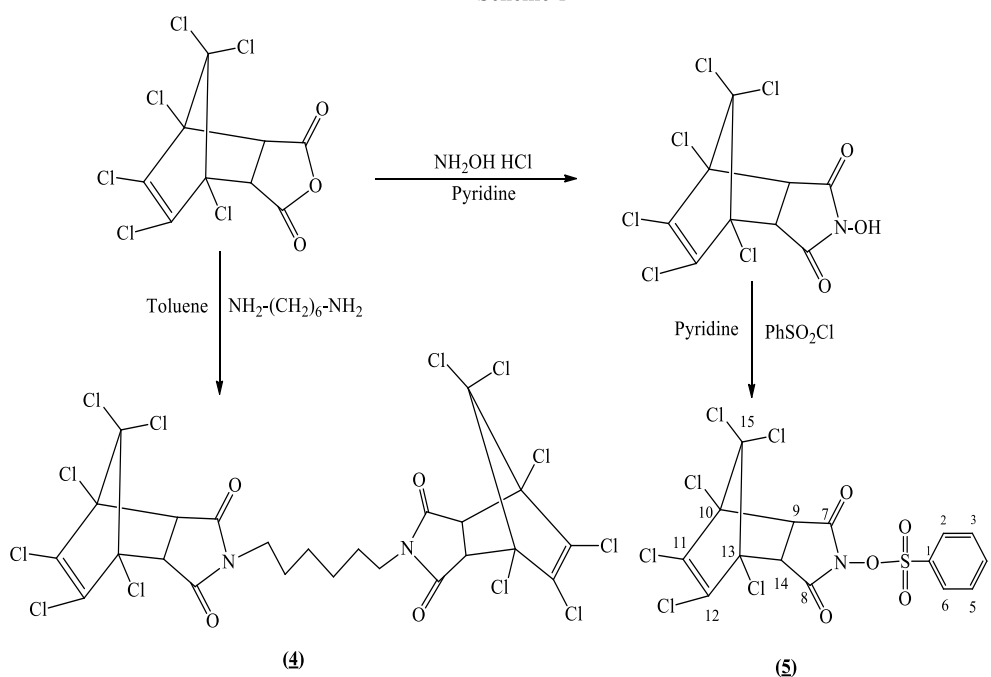
3.1. Characterization of the synthesized pyrrole derivatives

In this current work new pyrrole derivatives were formed via reaction of (11S,15R)-9,10,11,15-tetrahydro-9,10-[3,4]furanoanthracene-12,14-dione with sulfanilamide with 1:1 to give compound (**1**), and allowed to react with anthracen-9(10H)-ylidenhydrazine compound (**2**) which synthesized by reaction of anthrone with hydrazine hydrate to afford compound (**3**) scheme 1. FTIR spectra for these compounds showed bands in the region 1650 to 1776 expected for coupling carbonyl bands of cyclic imides, FTIR spectra of compound (**1**) indicates appearance of two bands due to νNH_2 at 3342, 3259 cm^{-1} . $^1\text{H-NMR}$ spectra of compound (**2**) show the presence of a singlet at δ 4.79 due to amino group in addition to the appearance of a multiplet at δ 7.12-8.34 for aromatic protons. $^1\text{H-NMR}$ spectra of compound (**3**) revealed to presence of a singlet at δ 3.44 (2H, CH_2 - anthrone), singlet at δ 3.65 (2H, 2CH sp^3), singlet at δ 4.87 (2H, 2CH sp^3) in addition to a multiplet at δ 6.66-7.79 for 16H, aromatic protons.

Scheme 2 indicated that Hexachloro-5-norbornene-2,3-dicarboxylic anhydride was reacted with hexamethylene diamine to afford compound (**4**). FTIR spectra of compound (**4**) indicates sharp band at 2861cm^{-1} for CH_2 -aliphatic and two bands for carbonyl groups in the range $1700\text{-}1781 \text{cm}^{-1}$. Also, FTIR spectra of compound (**5**) indicate to distinct band for $\text{SO}_2\text{-O-}$ at $1397, 1195 \text{cm}^{-1}$. $^1\text{H-NMR}$ spectra for compound (**4**) indicates the presence of a multiplet at δ 1.25(4H, 2CH_2) and a multiplet at δ 1.38(4H, 2CH_2) in addition to the appearance of a triplet at δ 3.32 (4H, $2\text{CH}_2\text{-N}$), figure 2. $^1\text{H-NMR}$ spectra of compound (**5**) show that appearance of a singlet at 4.28 for 2CH-SP^3 in addition to aromatic protons due to benzene ring, figure 3.



Scheme 1



Scheme 2

3.2 Electrochemical studies

3.2.1 Potentiodynamic polarization measurements.

The potentiodynamic polarization curves for carbon steel in 1.0 M HCl, in the absence and presence of different concentrations from compound **(2)** and compound **(4)** are illustrated in Figures 1,2. Similar curves (not shown) were obtained from the other compounds. Tafel polarization plots were obtained using scan rate of 1 mV s^{-1} in the potential range from -800 to +1 000 mV with respect to the open circuit potential (E_{ocp}) at 25°C . The calculated electrochemical parameters [corrosion potential (E_{corr}), anodic (β_a) and cathodic (β_c) Tafel slopes, corrosion current density (i_{corr}), and inhibition efficiency (%IE)] are calculated and given in Table 1.

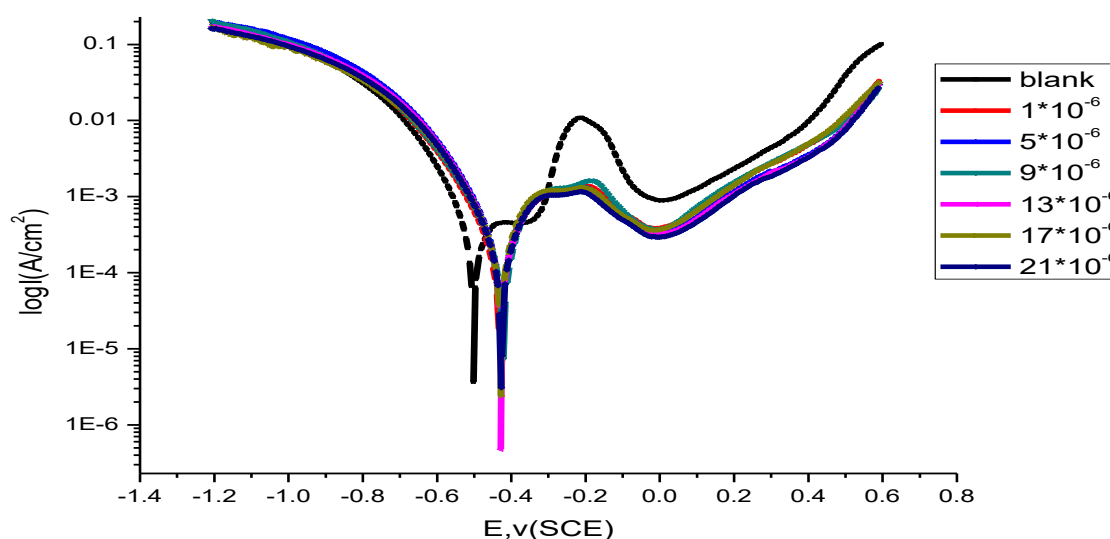


Figure 1. Potentiodynamic polarization curves for carbon steel in 1.0 M HCl solutions containing different concentrations of compound **(2)** at 25 °C

It is clearly seen from Table 1 that the values of i_{corr} decreased and the %IE increased in the presence of pyrrole derivatives. This effect significantly increased with increasing concentrations of pyrrole derivatives and attained a maximum inhibition 82.8% at 21×10^{-6} M for compound **(1)**. We can rank compounds according to their efficiency as follow: **(1)** > **(3)** > **(5)** > **(4)** > **(2)**. The inhibition efficiency was calculated from this equation:

$$\% \text{IE} = (I^0 - I^i) / I^0 \times 100 \quad (1)$$

where, I^0 and I^i are the corrosion current density in the absence and in the presence of inhibitor, respectively. The values of β_c and β_a are not significantly affected by changing the concentration of the compounds. This demonstrates that the compounds block the anodic and cathodic active sites within the covered fraction of the electrode surface and the mechanism of the corrosion reaction not affected [18-20]. From Table 1 the values of E_{corr} slightly shift to more positive potentials by increasing the concentration of inhibitors. These results indicate that these inhibitors act as a mixed-type inhibitors which act predominately on the anodic dissolution of the metal [21].

Table 1. Potentiodynamic polarization parameters for carbon steel in 1.0 M HCl solutions in the absence and presence of different concentrations of the compounds at 25 °C

Compounds	Conc.,(M)	$-E_{\text{corr}}$ mV vs. SCE	i_{corr} $\mu\text{A cm}^{-2}$	β_a mV dec^{-1}	$-\beta_c$ mV dec^{-1}	θ	%IE	mpy
(1)	Blank	502.0	640	247.8	124.3			261.30
	1×10^{-6}	469.0	301	244.4	113.0	0.530	53.0	137.6
	5×10^{-6}	467.0	250	246.1	115.1	0.601	60.1	118.6
	9×10^{-6}	461.0	206	255.6	114.5	0.678	67.8	98.5

	13x10 ⁻⁶	459.0	150	242.9	123.7	0.765	76.5	97.1
	17x10 ⁻⁶	457.0	130	243.2	111.8	0.797	79.7	95.3
	21x10 ⁻⁶	456.0	110	242.5	114.6	0.828	82.8	71.2
(2)	1x10 ⁻⁶	495.0	450	244.5	124.7	0.297	29.7	244.5
	5x10 ⁻⁶	494.0	433	245.4	126.0	0.323	32.3	231.6
	9x10 ⁻⁶	493.0	401	420.1	125.0	0.373	37.3	222.3
	13x10 ⁻⁶	492.0	370	249.4	123.4	0.422	42.2	207.9
	17x10 ⁻⁶	490.0	340	250.8	127.2	0.468	46.8	205.8
	21x10 ⁻⁶	488.0	330	248.8	118.8	0.484	48.4	190.2
(3)	1x10 ⁻⁶	479.0	393	249.1	129.9	0.386	38.6	179.7
	5x10 ⁻⁶	477.0	339	247.2	120.6	0.470	47.0	154.8
	9x10 ⁻⁶	475.0	250	430.7	128.4	0.609	60.9	154.0
	13x10 ⁻⁶	472.0	190	452.2	128.9	0.703	70.3	141.7
	17x10 ⁻⁶	470.0	170	243.2	121.2	0.734	73.4	127.1
	21x10 ⁻⁶	467.0	140	244.0	115.2	0.781	78.1	85.1
(4)	1x10 ⁻⁶	491.0	445	241.0	116.0	0.304	30.4	235.80
	5x10 ⁻⁶	491.0	410	250.0	127.8	0.359	35.9	230.0
	9x10 ⁻⁶	489.0	300	240.0	123.0	0.531	53.1	219.0
	13x10 ⁻⁶	488.0	260	245.7	115.5	0.594	59.4	204.7
	17x10 ⁻⁶	487.0	200	242.9	120.5	0.688	68.8	198.5
	21x10 ⁻⁶	485.0	180	246.2	110.1	0.718	71.8	177.0
(5)	1x10 ⁻⁶	489.0	424	258.2	130.4	0.337	33.7	190.1
	5x10 ⁻⁶	487.0	355	237.5	144.5	0.445	44.5	188.7
	9x10 ⁻⁶	485.0	290	256.1	125.0	0.547	54.7	179.3
	13x10 ⁻⁶	484.0	241	243.9	136.8	0.623	62.3	172.3
	17x10 ⁻⁶	482.0	192	248.1	120.4	0.700	70.0	168.4
	21x10 ⁻⁶	480.0	170	242.9	137.3	0.734	73.4	159.8

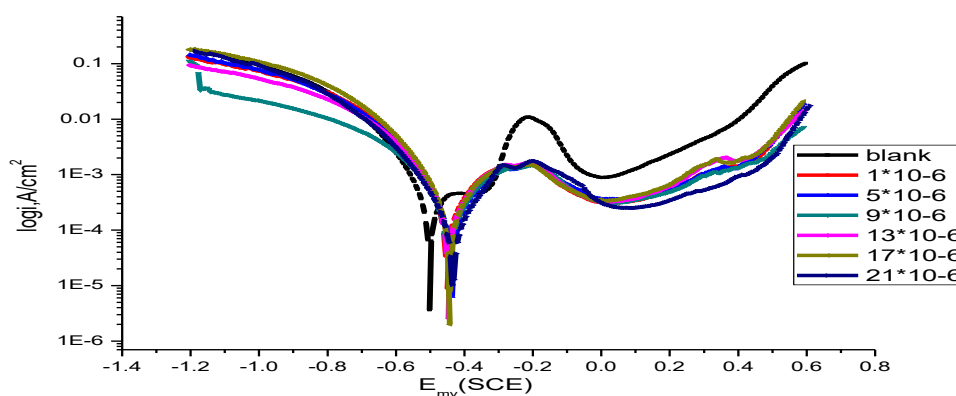


Figure 2. Potentiodynamic polarization curves for carbon steel in 1.0 M HCl solutions containing different concentrations of compound (4) at 25 °C

3.2.2 Electrochemical impedance spectroscopy.

EIS technique gives data on the resistive and capacitive behavior at the interface and makes it possible to estimate the performance of the test compound as a corrosion inhibitor [22-25].

The Nyquist and Bode plots obtained for carbon steel electrode in 1.0 M HCl solution in the absence and presence of various concentrations of compounds **(2)** and **(4)** at 25 °C are shown in Figures(3-6).

Also curves (not shown) were obtained for the rest compounds. Electrochemical impedance spectroscopy was studied at corrosion potentials, E_{corr} , over a frequency range of 10^5 Hz to 0.1 Hz with a signal amplitude perturbation of 10 mV. Nyquist plots consist of capacitive depressed semicircles and this refers to as frequency dispersion. This frequency dispersion may be as a result of the roughness of the solid surface [25]. The appearance of the capacitive semicircles indicates that the corrosion of carbon steel in 1.0 M HCl solutions in the absence and presence of pyrrole derivatives is under charge-transfer control [26]. When the pyrrole derivatives added to acid solution the diameter of the semicircle increases and hence charge transfer resistance (R_{ct}) of the corrosion reaction increases [27,28]. Increasing the concentration of the pyrrole derivatives in HCl solutions does not change substantially the shape of the semicircles confirming that these compounds do not alter the mechanism of the corrosion reaction but inhibits the corrosion processes via increasing the surface coverage of the electrode surface by an isolating adsorption layer of compounds. The simple equivalent circuit shown in Figure 7 was modeled to fit the EIS data [29]. This circuit consists of a parallel combination of a constant phase element (CPE) and the charge transfer resistance (R_{ct}) in series connection with the solution resistance (R_s).

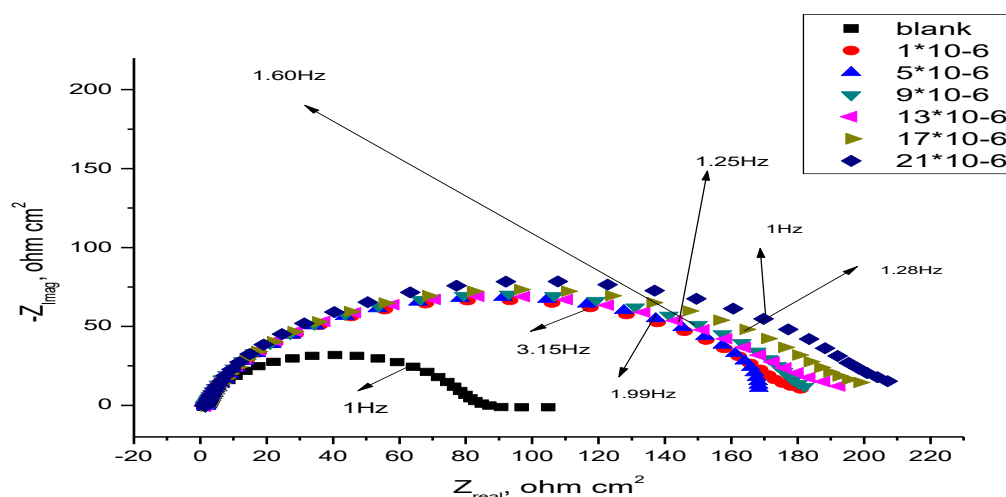


Figure 3. Carbon steel Nyquist plots in 1.0 M HCl solutions in the absence and presence of different concentrations of compound **(2)** at 25 °C.

We used the CPE element instead of the pure capacitor to reduce the effect of the roughness and the presence of adsorbed inhibitors species on the surface of the electrode [30]. CPE element represents the double layer capacitance (C_{dl}). The admittance and impedance of the CPE can be defined from the following equation [31,32].

(2)

where Y_0 is the magnitude of CPE, $j^2 = -1$ is the imaginary number ω is the sine wave modulation angular frequency ($\omega = 2\pi f$, where f is the A C frequency). In actual experimental conditions, the values of n are between 0 and 1 due to the influence of different factors such as

electrode roughness, surface heterogeneity, and the dielectric constant [33]. The values of C_{dl} can be calculated using eqn. [34-36].

$$C_{dl} = Y_0^{1/n} R_{ct}^{(1-n)/n} \quad (3)$$

By the following equation the inhibition efficiencies (IE) were calculated for different concentrations of pyrrole derivatives at 25 °C:

$$\%IE = R_{ct}^0 - R_{ct} / R_{ct} \quad (4)$$

where R_{ct}^0 and R_{ct} are the charge-transfer resistance values in uninhibited and inhibited solutions respectively.

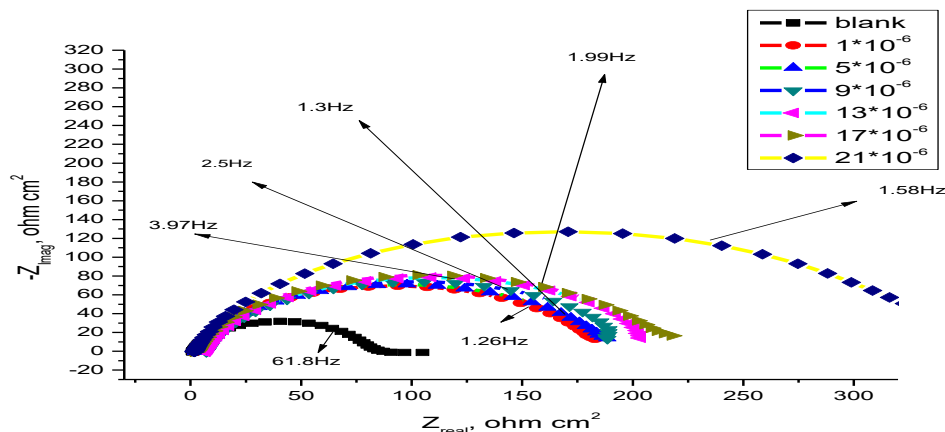


Figure 4. Carbon steel Nyquist plots in 1.0 M HCl solutions in the absence and presence of different concentrations of compound (4) at 25 °C.

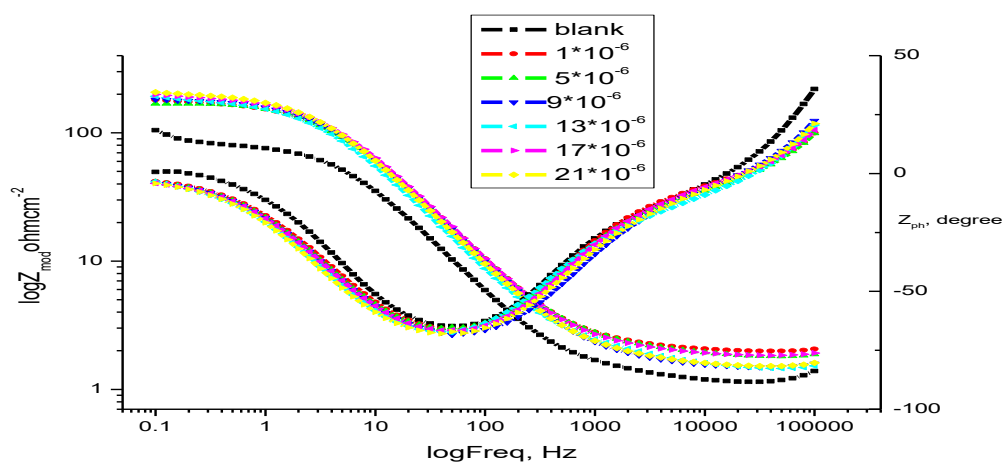


Figure 5. Carbon steel Bode plots in 1.0 M HCl solutions in the absence and presence of different concentrations of compound (2) at 25 °C

The data which listed in Table2, demonstrates that the value of R_{ct} increases while that of C_{dl} decreases with increasing the concentrations of compounds. This result from a decrease in local dielectric constant and /or an increase in the thickness of the electrical double layer. This happens when compounds adsorb at the metal/solution interface [37]. The inhibition efficiency of compounds increases with increasing their concentrations in the acid solution.

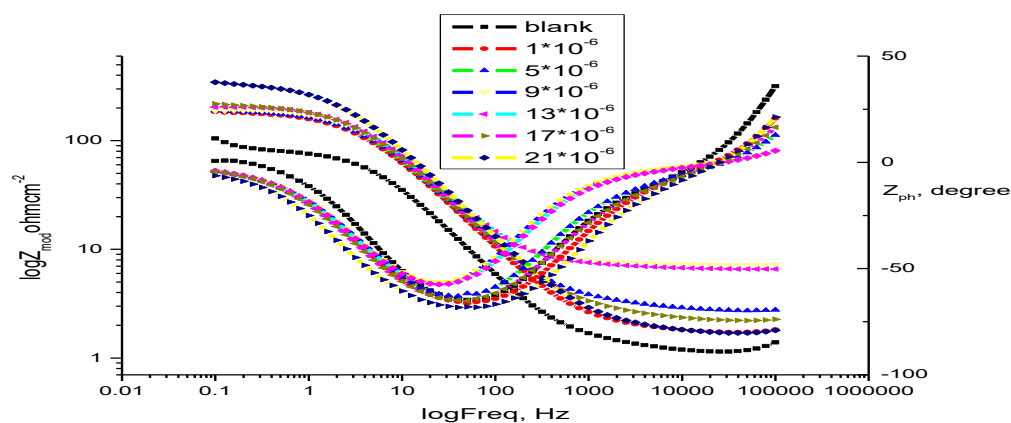


Figure 6. Carbon steel Bode plots in 1.0 M HCl solutions in the absence and presence of different concentrations of compound (4) at 25°C

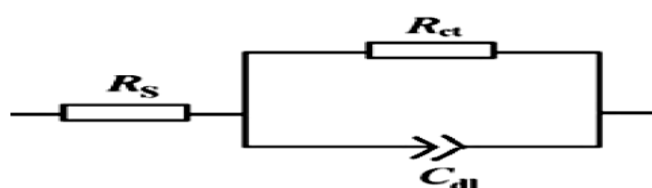


Figure 7. Equivalent circuit proposed to fit the EIS experimental data

3.2.3 Electrochemical frequency modulation (EFM).

EFM technique was used for showing the behavior of carbon steel corrosion in 1.0 M HCl without and with different concentrations of inhibitors at 25 °C. The results of EFM experiments are a spectrum of current response as a function of frequency. The spectrum is called the intermodulation spectrum. Figure 8 shows intermodulation spectrum of carbon steel in 1.0 M HCl and 1.0 M HCl containing 21×10^{-6} M from compounds (2) and (4) (as representative examples).

Similar results were recorded for the other inhibitors concentrations. The spectra contain current responses assigned for harmonical and intermodulation current peaks. The larger peaks were used to calculate the corrosion current density (I_{corr}), the Tafel slopes (β_a and β_c) and the causality factors (CF-2 and CF-3). These corrosion kinetic parameters were determined by applying potential perturbation signal with amplitude 10 mV with two sine waves of 2 and 5 Hz. The choice for the frequencies of 2 and 5 Hz was based on three arguments[38]. Table 3 demonstrates that, the corrosion current densities decrease by increasing the concentrations of the studied compounds. The inhibition efficiency (%IE) and the degree of surface coverage (θ) increase by increasing the studied inhibitors concentrations and were calculated from the data obtained from EFM measurement using the following equation:

$$\% \text{IE} = (I^0 - I^i) / I^0 \times 100 \quad (5)$$

where I^0 and I^i are defined previously in eqn (1).

Table 2. EIS parameters for corrosion of carbon steel in 1.0 M HCl in the absence and presence of different concentrations of inhibitors at 25 °C

Compounds	Conc., (M)	R_{ct} , Ωcm^{-2}	R_s , Ωcm^{-2}	Y^0X10^6 , $\mu\Omega^{-1}\text{S}^n$	n	$C_{dl} \times 10^4$, F cm^{-2}	θ	%IE
	Blank	79.5	1.934	434.8	0.933	3.40		
(1)	1×10^{-6}	239.00	1.860	379.0	0.839	2.39	0.666	66.6
	5×10^{-6}	244.70	2.020	519.0	0.780	2.90	0.675	67.5
	9×10^{-6}	348.30	1.990	380.3	0.818	2.42	0.772	77.2
	13×10^{-6}	395.10	1.820	345.6	0.807	2.14	0.798	79.8
	17×10^{-6}	419.90	1.870	320.0	0.749	2.13	0.811	81.1
	21×10^{-6}	447.10	1.830	318.0	0.825	2.10	0.822	82.2
(2)	1×10^{-6}	111.10	2.020	422.5	0.855	2.67	0.284	28.4
	5×10^{-6}	114.20	1.880	435.0	0.839	2.65	0.304	30.4
	9×10^{-6}	180.90	1.920	422.9	0.853	2.64	0.561	56.1
	13×10^{-6}	185.30	1.950	537.0	0.833	3.38	0.571	57.1
	17×10^{-6}	191.70	1.880	413.0	0.849	2.63	0.585	58.5
	21×10^{-6}	203.80	1.960	408.0	0.849	2.62	0.610	61.0
(3)	1×10^{-6}	220.00	1.889	550.0	0.859	3.31	0.639	63.9
	5×10^{-6}	225.00	1.948	403.9	0.835	2.51	0.646	64.6
	9×10^{-6}	236.30	1.984	426.5	0.824	2.60	0.664	66.4
	13×10^{-6}	293.60	1.759	344.3	0.841	2.23	0.729	72.9
	17×10^{-6}	347.60	1.792	319.2	0.845	2.13	0.772	77.2
	21×10^{-6}	436.40	1.782	293.1	0.844	2.00	0.820	82.0
(4)	1×10^{-6}	112.10	1.757	439.4	0.839	2.70	0.290	29.0
	5×10^{-6}	118.00	1.847	447.7	0.828	2.67	0.330	33.0
	9×10^{-6}	189.20	1.912	400.5	0.844	2.49	0.580	58.0
	13×10^{-6}	203.60	1.823	402.4	0.836	2.46	0.607	60.7
	17×10^{-6}	215.40	1.890	405.2	0.827	2.43	0.631	63.1
	21×10^{-6}	337.60	1.734	354.5	0.838	2.35	0.765	76.5
(5)	1×10^{-6}	120.00	1.900	480.0	0.868	2.95	0.338	33.8
	5×10^{-6}	126.90	1.980	487.1	0.832	2.77	0.374	37.4
	9×10^{-6}	198.00	1.810	440.2	0.830	2.67	0.598	59.8
	13×10^{-6}	270.00	1.980	410.0	0.830	2.61	0.706	70.6
	17×10^{-6}	310.00	1.990	399.4	0.831	2.60	0.744	74.4
	21×10^{-6}	350.00	1.950	390.3	0.828	2.58	0.773	77.3

Causality factor has great strength of the EFM technique, which serves as an internal check on the validity of the EFM measurement [39]. The values of causality factors in Table 3 indicate that the measured data are of good quality. The standard values for CF-2 and CF-3 are 2.0 and 3.0, respectively. If the causality factors differ significantly from the theoretical values of 2.0 and 3.0, then it can be deduced that the measurements are influenced by noise. If the causality factors are approximately equal to the predicted values of 2.0 and 3.0, and EFM technique is reliable for monitoring of carbon steel corrosion in the blank and the inhibited solutions[40]. The results obtained by different techniques are showed similar behavior. The variations of the inhibition efficiencies (%)

IE) are attributed to the variations between the individual techniques and the various models that were used for the interpretation [38,41].

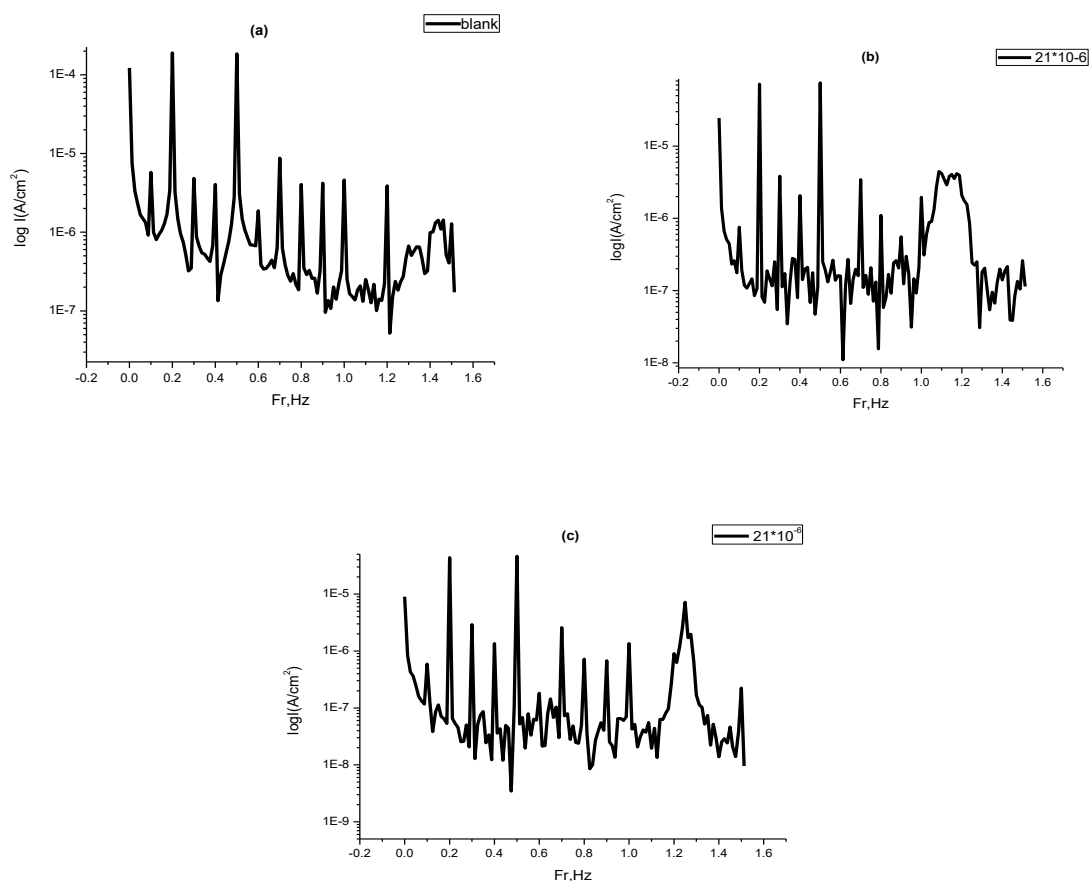


Figure 8. Intermodulation spectrum for the corrosion of carbon steel electrode in 1.0 M HCl solution alone (a), and intermodulation spectra for the corrosion of carbon steel in 1.0M HCl solution containing 21×10^{-6} M of compound (**2**) (b) and 1.0M HCl solution containing 21×10^{-6} M of compound (**4**) (c) at 25°C

Table 3. Electrochemical parameters for carbon steel determined from EFM measurements in 1.0 M HCl solution without and with the addition of various concentrations of pyrrole derivatives at 25°C

Compounds	Conc.,(M)	i_{corr} $\mu\text{A cm}^{-2}$	β_a mV dec^{-1}	$-\beta_c$ mV dec^{-1}	CF-2	CF-3	θ	%IE
(1)	blank	216.80	69.53	82.22	1.57	2.83	-----	-----
	1×10^{-6}	111.8	100.3	132.0	1.99	2.99	0.484	48.4
	5×10^{-6}	78.05	106.7	168.3	2.03	2.67	0.640	64.0
	9×10^{-6}	73.92	96.06	131.8	2.18	3.20	0.659	65.9
	13×10^{-6}	60.67	99.28	142.5	1.94	3.39	0.720	72.0
	17×10^{-6}	52.39	106.5	133.2	2.14	3.23	0.758	75.8
	21×10^{-6}	37.96	177.9	179.9	1.31	3.80	0.824	82.4

(2)	1×10^{-6}	154.8	100.6	145.6	2.0	2.46	0.290	29.0
	5×10^{-6}	144.6	86.17	123.2	1.92	3.73	0.333	33.3
	9×10^{-6}	134.8	91.0	126.4	2.2	3.20	0.380	38.0
	13×10^{-6}	127.3	93.8	129.5	1.35	2.98	0.413	41.3
	17×10^{-6}	125.2	91.97	120.2	1.56	3.42	0.422	42.2
	21×10^{-6}	109.4	84.2	112.9	1.82	3.30	0.495	49.5
(3)	1×10^{-6}	130.3	19.15	21.060	2.50	3.10	0.399	39.9
	5×10^{-6}	114.5	90.6	130.20	2.70	3.40	0.472	47.2
	9×10^{-6}	110.9	97.76	132.60	2.40	3.50	0.488	48.8
	13×10^{-6}	70.9	89.66	125.90	2.50	2.70	0.673	67.3
	17×10^{-6}	54.09	85.77	125.00	1.77	2.97	0.750	75.0
	21×10^{-6}	52.13	61.46	74.94	2.07	3.20	0.760	76.0
(4)	1×10^{-6}	147.40	99.07	140	2.097	3.62	0.32	32.0
	5×10^{-6}	142.60	94.55	133.9	2.019	2.94	0.35	35.0
	9×10^{-6}	82.14	63.68	78.04	2.34	3.77	0.62	62.0
	13×10^{-6}	80.14	59.00	70.27	2.19	3.33	0.63	63.0
	17×10^{-6}	73.66	62.54	76.29	2.05	3.09	0.66	66.0
	21×10^{-6}	65.58	80.66	115.7	2.03	3.55	0.697	69.7
(5)	1×10^{-6}	145.5	56.7	67.9	1.91	3.01	0.329	32.9
	5×10^{-6}	140.0	63.2	99.1	1.82	3.40	0.354	35.4
	9×10^{-6}	80.0	79.4	88.6	1.99	3.20	0.631	63.1
	13×10^{-6}	78.5	80.4	111.3	1.67	2.99	0.638	63.8
	17×10^{-6}	70.5	81.3	100.5	1.78	2.97	0.675	67.5
	21×10^{-6}	61.18	89.3	120.5	1.88	2.79	0.715	71.5

3.2.4 Adsorption isotherm

The inhibition results which obtained in aggressive acid media is assumed to be due to its adsorption at the metal /solution interface. The mode of adsorption will be dependent on factors such as the composition of compounds, chemical changes to the compounds and the nature of the surface charge on metal. An anion adsorption is favored by a positive surface charge and vice versa. In order to obtain the adsorption isotherm, the degree of surface coverage (θ) of the compounds must be calculated. To determine the adsorption mode, there are a number of mathematical expressions having thus developed to take into consideration of non-ideal effects. The most used isotherms are Frumkin, De Boer, Parsons, Temkin, Flory-Huggins and Bockris-Swinkels [42-45]. Figure13 indicating that the inhibitors obey Langmuir adsorption isotherm given by the equation [46]:

$$C/\theta = 1/K_{ads} + C \quad (6)$$

where C is the molar concentration of inhibitors, K_{ads} is the equilibrium constant of the adsorption process and θ is the degree of coverage by molecules of inhibitors on the metal surface. The straight line is obtained when C/θ is plotted against C and the linear correlation coefficient of the fitted data is close to 1.

The obtained values of K_{ads} are listed in Table4. The K_{ads} value could takes as a measure of the strength of the adsorption forces between the metal surface and the molecules of inhibitor. The higher values of K_{ads} , suggested that the inhibitor performed stronger adsorption ability onto the carbon steel

surface. By using the following equation we can get the values of the standard Gibbs free energy of adsorption (ΔG_{ads}) [47]:

$$K_{\text{ads}} = 1/55.5 \exp(-\Delta G_{\text{ads}}/RT) \quad (7)$$

Where R is the universal gas constant, T is the thermodynamic temperature and 55.5 is the concentration of water in the solution in mol / l.

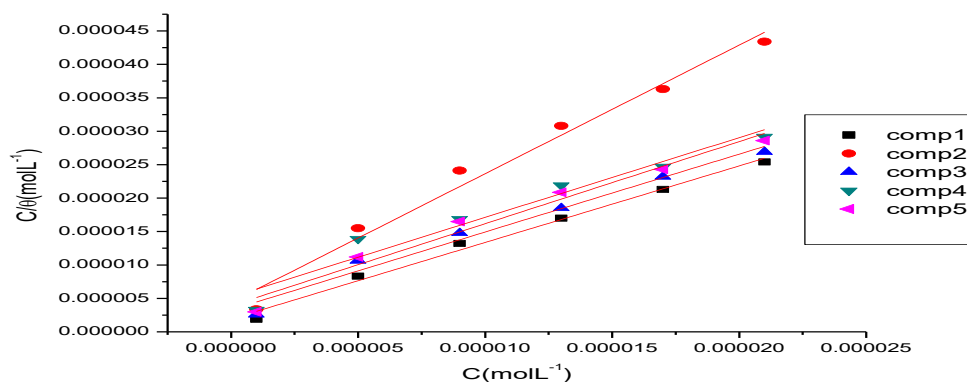


Figure 9. Langmuir's isotherm adsorption model for different compounds on the carbon steel surface in 1.0M HCl solutions .

Table 4. Langmuir adsorption parameters for adsorption of inhibitors on carbon steel in 1.0 M HCl

Compounds	Langmuir isotherm		
	Log K M ⁻¹	R ²	-ΔG _{ads} KJmol ⁻¹
(1)	5.72	0.99	42.6
(2)	5.35	0.98	40.5
(3)	5.48	0.98	41.2
(4)	5.28	0.94	40.1
(5)	5.41	0.97	40.8

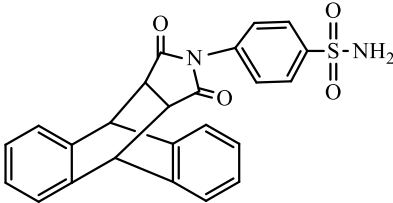
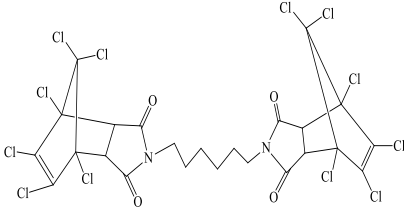
The negative values of ΔG_{ads} reveal the spontaneity of the process of adsorption and also reveal to the stability of the adsorbed layer on the carbon steel surface. Theoretically, the values of ΔG_{ads} around -20 kJ mol⁻¹ or more positive are consistent with physisorption, while those around -40 kJ mol⁻¹ or more negative with chemisorption [48]. The values of ΔG_{ads} are in the range from -40.1 to -42.6 kJ mol⁻¹, which automatically reflects that the adsorption mechanism of compounds on carbon steel in the 1.0M HCl solution corresponds to a chemisorption (Table 4).

3.2.5 Analysis of FT-IR spectra:

To identify the functional groups present in inhibitors we used FTIR analysis. The FTIR spectra of the compounds **(1)**, **(4)** are presented in Table 5. Table 5 demonstrates IR spectra of compounds **(1),(5)** as a solid and in 1.0 M HCl before adsorption on carbon steel and after adsorption on carbon steel surface (FTIR spectra of other compounds studied not shown). The results obtained

show that corrosion inhibition takes place through adsorption process. There is a shift in the spectra of the compounds **(1)**, **(4)** when carbon steel was immersed in it to form corrosion product. This shows that there is an interaction between the inhibitor and the carbon steel substrate which resulted in inhibition. The shifts in the spectra consider as a result of the interaction between the inhibitor and carbon steel occurred through the functional groups presents in them. So, it can be affirmed that the functional group of inhibitor has coordinated with Fe^{2+} formed on the metal surface resulting in the formation of Fe^{2+} inhibitor complex on the metal surface, which promotes the inhibition of the metal sample[49].

Table 5 the data of IR spectra of compounds **(1)** and **(4)** as a solid and in 1.0M HCl without carbon steel (before) and after immersion carbon steel for 24h (after).

Compounds	Groups	Wavenumber (cm^{-1}) (solid)	Wavenumber (cm^{-1}) (before)	Wavenumber (cm^{-1}) (after)
 <p>(1)</p>	NH ₂	3342-3259	3367.1	3399.89
	C-H	2969	2983.34	2983.34
	aromatic			
	C=O	1776-1650	1650.77	1652.7
	S=O	1498	1420.52	1467.56
	C=C	1610	1390.24	1390.42
	aromatic			
 <p>(4)</p>	C-N	1317	1278.57	1255.43
	C=O	1781-1700	1720-1610	1710-1600
	C=C	1598	1562	1500
	aromatic			
	C-N	1155	1087	1010
	aliphatic			

3.2.6 UV-visible analysis

Visible absorption spectra obtained from 1.0 M HCl solution containing $21 \times 10^{-6} \text{M}$ compound **(4)** before and after the carbon steel immersion are shown in Figures 10,11 which confirmed the possibility of the formation of inhibitor-Fe complex. The electronic absorption spectra of compound **(4)** before immersion have absorption maximum at 215nm which can be attributed to π - π^* and n-transitions[50]. After 24hrs immersion of carbon steel, there is a change in the absorbance values and change in the position of absorption maximum indicates that the complex formation between two species in solution[51]. These experimental findings provide the formation of complex between Fe^{2+} and compound **(4)** and confirm the inhibition of steel from corrosion. (The same results obtained from the other compounds).

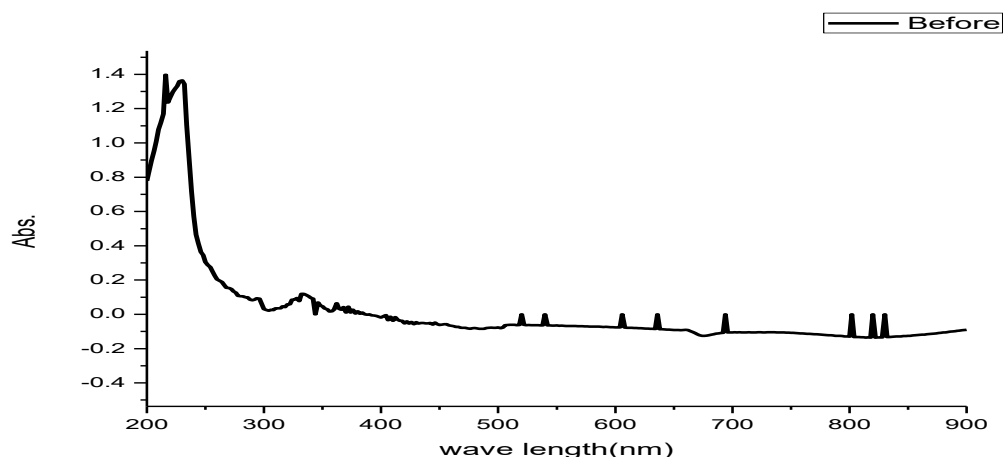


Figure 10. UV-Visible spectra of the solution from 1.0 M HCl solution containing 21×10^{-6} M from compound **(4)** before carbon steel immersion

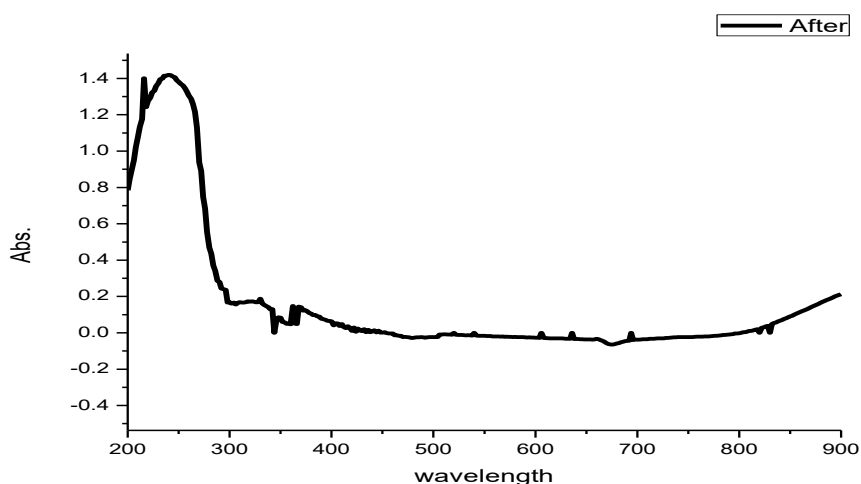


Figure 11. UV-Visible spectra of the solution from 1.0 M HCl containing 21×10^{-6} M from compound **(4)** after 24h of carbon steel immersion

3.3. Mechanism of inhibition

The adsorption of pyrrole derivatives compounds can be attributed to the presence of polar units having atoms of nitrogen, sulphur, oxygen and aromatic/heterocyclic rings. Therefore, the possible reaction centers are unshared electron pair of hetero-atoms and π electrons of aromatic ring.

The adsorption and inhibition effect of pyrrole derivatives compounds in 1.0 M HCl solution can be explained as follows:

The neutral molecules may be adsorbed on the surface of alloy through the chemisorption mechanism, involving the displacement of water molecules from the alloy surface and the sharing electrons between the hetero-atoms and metal. The inhibitor molecules can also adsorb on the alloy surface on the basis of donor-acceptor interactions between π electrons of the aromatic ring and vacant d-orbitals of surface iron atoms.

The order of inhibition is decreased as the following order: 1 > 3>5>4>2. This due to the difference in number of nitrogen atoms, oxygen atoms and sulphur atoms in the compounds, which increase the electron charge density on the molecule.

4. CONCLUSIONS

The results obtained show that pyrrole derivatives are good corrosion inhibitors for carbon steel under acidic conditions. The maximum inhibition efficiency was 82.8% for compound (**1**). Excellent agreement between the inhibition efficiencies calculated using different techniques was obtained. The adsorption of the Pyrrole derivatives onto the steel surface was characterized by the decrease in: (i) the cathodic and anodic current densities observed in the potentiodynamic polarization curves carried out in the presence of pyrrole derivatives, (ii) the double-layer capacitance computed from electrochemical impedance spectroscopy experiments and (iii) electrochemical frequency modulation (EFM). The adsorption behavior of the Pyrrole derivatives are consistent with Langmuir adsorption isotherm. Inhibitors are adsorbed on Carbon steel surface following chemisorption mechanism. The results of polarization indicated that compounds are of mixed type. A good agreement was obtained between all the investigated electrochemical techniques. The results obtained from FTIR, UV-visible analysis and Langmuir adsorption isotherm suggested that the mechanism of corrosion inhibition is occurring mainly through adsorption process.

References

1. M. Yadav, D. Behera, S. Kumar and R. R. Sinha, *Ind. Eng. Chem. Res.*, 52(2013) 6318.
2. Y. M. Tang, X. Y. Yang, W. Z. Yang, R. Wan, Y. Z. Chen and X. S. Yin, *Corros. Sci.*, 52(2010) 1801.
3. M. B. Cisse, B. Zerga, F. El Kalai, M. Ebn Touhami, M. Sfaira, M. Taleb, B. Hammouti, N. Benchat, S. El Kadiri and A. T. Benjelloun, *Review and Letters*, 18(2011)303.
4. A. Y. Musa, R. T. T. Jalgham and A. B. Mohamad, *Corrosion Science*, 56(2012) 176.
5. S. E. Nataraja, T. V. Venkatesha and H. C. Tandon, *Corrosion Science*, 60(2012) 214.
6. E. A. Noor, A. H. Al-Moubaraki, *Mater. Chem. Phys.*, 110(2008) 145.
7. Y. El Kacimi, R. Touri, M. Galai, R. A. Belakhmima, A. Zarrouk, K. Alaoui, M. Harcharras, H. El Kafssaoui and M. Ebn Touhami, *J. Mater. Environ. Sci.*, 7(2016) 371.
8. S. T. Keera and M. A. Deyab, *Colloids Surf. A: Physicochem. Eng. Aspects*, 266(2000)129.
9. A. Chetouani, B. Hammouti, T. Benhadda and M. Daoudi, *Appl. Surf. Sci.*, 249(2005), 375.
10. B. P. Etherton, R. Krishnamurti and S. Nagy, *US patent*, (5)554(1996)775.
11. A. Kaledkowski and A. W. Trochimczuk, *React. Funct. Polym.*, 66 (2006) 740.
12. Y. Zhu, A. Rabindianath, T. Beyerlein and B. Tieke, *Macromolecules*, 40(2007) 6981.
13. H. Lee, J. Lee, S. Lee, Y. Shin, W. Jung, J. H. Kim, K. Park, K. Kim, H. S. Cho and S. Ro. *Bioorg. Med. Chem. Lett.*, 11(2001) 3069.
14. D. O. Hagan, *Nat. Prod. Rep.*, 17(2000)435.
15. V. J. Gelling, M. M. Wiest, D. E. Tallman, G. P. Bierwagen and G. G. Wallace, *Prog. Org. Coat.*, 43(2001)149.
16. K. M. Govindaraju, V. Collins Arun Prakash and V. Manivannan L. Kavitha, *J Appl Electrochem.*, 39(2009)269.
17. A. Zarrouka, B. Hammoutia, T. Lakhlib, M. Traisnelc, H. Vezind and F. Bentissc, ASTM, G 31–72, American Society for Testing and Materials, Philadelphia, PA, 1990.

18. J. Aljourani, K. Raeissi, M. A. Golozar, *Corros. Sci.*, 51(2009)1836.
19. H. M. Abd El-Lattef, V. M. Abbasov, L. I. Aliyeva, E. E. Qaismov and I.T. Ismayilov, *Mater. Chem. Phys.*, 142(2013)502.
20. R. Mehdaoui, A. Khelifa, A. Khadraoui, O. Aaboubi, A. Hadj Ziane, F. Bentiss and A. Zarrouk, *Res Chem Intermed*, 42(2016)5509.
21. I. Ahamad and M. Quraishi, *Corros. Sci.*, 51(2009) 2006.
22. S. Zhang, Z. Tao, W. Li and B. Hou, *Appl. Surf. Sci.*, 255(2009) 6757.
23. M. Outirite, M. Lagrenée, M. Lebrini, M. Traisnel, C. Jama, H. Vezin and F. Bentiss, *Electrochim. Acta*, 55(2010)1670.
24. G. E. Badr, *Corros. Sci.*, 51(2009) 2529.
25. M. Palomar-Pardavé, M. Romero-Romo, H. Herrera-Hernández, M. A. Abreu Quijano V. Natalya-Likhanova, J. Uruchurtu and J. M. Jurez-García, *Corros. Sci.*, 54(2012) 231.
26. K. F. Khaled and N. Hackerman, *Mater. Chem. Phys.*, 82(2003) 949.
27. F. Bentiss, M. Outirite, M. Traisnel, H. Vezin, M. Lagrenée, B. Hammouti, S. S. Al-Deyab and C. Jama, *Int. J. Electrochem. Sci.*, 7(2012) 1699.
28. I. Ahamad, R. Prasad and M. A. Quraishi, *Corros. Sci.*, 52(2010) 1472.
29. E. E. Oguzie, V. O. Njoku, C. K. Enenebeaku, C. O. Akalezi and C. Obi, *Corros. Sci.*, 50(2008) 3480.
30. M. Bouklah, B. Hammouti, M. Lagrenée and F. Bentiss, *Corros. Sci.*, 48(2006) 2831.
31. H. Ashassi-Sorkhabi and E. Asghari, *Electrochim. Acta*, 54(2008) 162.
32. B. D. Mert, A. O. Yüce, G. Kardas, and B. Yazıcı, *Corros. Sci.*, 85(2014) 287.
33. Z. Lukacs, *J. Electroanal. Chem.*, 68(1999) 464.
34. B. Hirschorn, M. E. Orazem, B. Tribollet, V. Vivier, I. Frateur and M. Musiani, *J. Electrochem. Soc.*, 157(2010) C458.
35. B. Hirschorn, M. E. Orazem, B. Tribollet, V. Vivier, I. Frateur and M. Musiani, *Electrochim. Acta*, 55(2010) 6218.
36. C. H. Hsu and F. Mansfeld, *Corrosion*, 57(2001) 747.
37. K. R. Ansari, M.A. Quraishi and A. Singh, *Corros. Sci.*, 79(2014) 5.
38. R. W. Bosch, W. F. Bogaerts and B. Syrett, Proc. 8th International Symposium on Electrochemical Methods in Corrosion Research modulation (EFM) technique, Nieuwpoort, Belgium, May 2003, 4–9
39. A. S. Fouda, A. A. Nazeer and A. Saber, *J. Korean Chem. Soc.*, 58(2)(2014) 160.
40. K. F. Khaled and N. S. Abdel-Shafi, *Int. J. Electrochem. Sci.*, 8(2013) 1409.
41. M. N. EL-Haddad and A. S. Fouda, *Chem Eng Comm*, 200(2013) 1366.
42. Z.M. Hadi and J. Al-Sawaad, *Mater. Environ. Sci.*, 2(2)(2011) 128.
43. P. N. G. Shankar and K. I. Vasu, *J. Electrochem. Soc. India*, 32(1983) 47.
44. A. Amin, K.F. Khaled, Q. Mohsen and A. Arida, *Corros. Sci.*, 52(2010)1684.
45. S. A. Umoren, O. Ogbo, I.O. Igwe and E. E. Ebenso, *Corros. Sci.*, 50(2008)1998.
46. R. Solmaza, G. Kardas, M. Culha, B. Yazıcı and M. Erbil, *Electrochim. Acta*, 53(2008) 5941.
47. Mahmoud N. El-Haddad, *RSC Adv.*, 6(2016) 57844.
48. A. K. Singh and M. A. Quraishi, *Corros. Sci.*, 53(2011) 1288.
49. S. S. Syed Abuthahir, A. Jamal Abdul Nasser and S. Rajendran, *Eur. Chem. Bull.*, 2(11)(2013) 932.
50. J. Jeyasundari, S. Rajendran, R. Sayee Kannan and Y. Brightson Arul Jacob, *Eur. Chem. Bull.*, 2(9)(2013) 585.
51. N.O. Obi-Egbedia and I.B. Obot, *Arabian Journal of Chemistry*, 6(2013) 211.